Marshall, S. A., "An Approximate Method for Reducing the Order of Linear Systems," *Control*, **10**, 642 (1966).
Meier, L., and D. Luenberger, "Approximation of Linear Constant Systems," *IEEE Trans. on Auto. Control*, **AC-12**, 585 (1967).
Moore, B. C., "Principal Component Analysis in Linear Systems: Controllability, Observability and Model Reduction," *IEEE Trans. on Auto. Control*, **AC-26**, 17 (1981). (see also earlier *System Control Reports 7,801, 7,802*, Dept. of EE, U. of Toronto, Canada.)
Nicholson, H., "Dynamic Optimization of a Boiler," *Proc. IEE*, **111**, 1,479 (1964).
Parthasarthy, R., K. N. Jayasimha, and S. John, "On Model Reduction by Modified Cauer Form," *IEEE Trnas. on Auto. Control*, **AC-28**(4), 523 (1983).
Riggs, J. B., and T. F. Edgar, "Least Squares Reduction of Linear Systems Using Impulse Response," *Int. J. Control*, **20**(2), 213 (1974).
Shamash, Y., "Model Reduction Using the Routh Stability Criterion and the Pade Approximation Technique," *Int. J. Control*, **21**, 475 (1975).
Sinha, N. K., and G. T. Bereznai, "Optimal Approximation of High Order System by Low Order Model," *Int. J. Control*, **14**, 951 (1971).
Shokoohi, S., L. M. Silverman, and P. M. Van Dooren, "Linear Time-Variable Systems: Balancing and Model Reduction," *IEEE Trans. on Auto. Control*, **AC-28**(8), 810 (1983).
Tsafestas, S. G., and P. N. Paraskevopouros, "On the Decoupling of Multivariable Control Systems with Time Delays," *Int. J. Control*, **17**, 405 (1973).
Tung, L. S., and T. F. Edgar, "Least Squares Model Reduction of Multiple Input-Multiple Output Linear Systems," *Proc. Joint Auto. Control Conf.*, Denver (1979).
Wilson, R. G., D. G. Fisher, and D. E. Seborg, "Model Reduction for Discrete Time Dynamic Systems," *Int. J. Control*, **16**, 549 (1972).
Wilson, R. G., D. E. Seborg, and D. G. Fisher, "Model Approach to Control Law Reduction," *Proc. Joint Auto. Control Conf.*, Columbus, OH, 554 (1973).
Wilson, R. G., "Model Reduction and the Design of Reduced Order Control Laws," Ph.D. Thesis, Univ. of Alberta (1974).
Wilson, R. G., D. G. Fisher, and D. E. Seborg, "Model Reduction and the Design of Reduced Order Control Laws," *AIChE J.*, **20**(6), 1,131 (1974).
Wilson, R. G., D. E. Seborg, and D. G. Fisher, "A Least Squares Approach to Model Reduction and the Design of Low-Order Controllers," *Can. J. Chem. Eng.*, **54**, 220 (June, 1976).

Manuscript received April 10, 1979; revision received April 17, 1984, and accepted April 30.

Taylor-Aris Dispersion Arising from Flow in a Sinusoidal Tube

An analysis of dispersion arising from creeping flow through a periodically constricted tube is developed with the goal of evaluating the effect of converging and diverging pore structure on dispersion in porous media. The theory is based on rigorous long-time solutions of the convective-diffusion equation. The calculations are done numerically over a range of Peclet numbers and tube geometries; for the geometrical parameters which correlate permeability data in packed beds, the results of the present work agree well with liteature data for dispersion in such beds.

D. A. HOAGLAND and R. K. PRUD'HOMME

Department of Chemical Engineering
Princeton University
Princeton, NJ 08544

SCOPE

Fluid motion in periodically constricted tubes has been studied by several authors interested in modeling flow through porous media. Using a model which replaces a porous medium with an equivalent array of periodically constricted tubes, these authors have been able to use flow-rate/pressure-drop relationships in the simpler geometry to successfully predict permeabilities of complex porous media. The dispersion of solute during flow through porous materials can be studied using the same geometrical models. The motivation for such modeling of dispersion lies in the crucial role of this phenomenon in oil recovery problems, reactor design, and chromatography. The present work will examine dispersion during creeping flow in a periodically constricted tube; it is proposed that the solution to this problem offers considerable insight into the dispersion processes observed during flow in more complex porous media.

The present work employs the concept of local and global coordinates which was developed by Brenner (1980) to describe transport in periodic structures and is an extension of earlier work of Taylor (1953) and Aris (1956). Using Brenner's analysis, this paper will describe the calculation of dispersion coefficients in sinusoidal tubes for wide ranges of Peclet number and tube geometry. Additionally, analytical solutions have been found to the limiting case of very long wavelength. The numerically determined dispersion coefficients can be compared to literature data for dispersion in packed beds if suitable geometrical parameters are selected. This comparison will test the hypothesis that dispersion in packed beds can be predicted with the same pore structure models used for correlating permeability data. It should be noted that transfer of solute between different flow channels has not been incorporated into the present model.

CONCLUSIONS AND SIGNIFICANCE

Dispersion coefficients for creeping flow in sinusoidal tubes have been calculated both analytically and numerically over wide ranges of tube geometry and Peclet number. The results have been obtained rigorously from long-time solutions of the

convective-diffusion equation. The numerical procedure employs collocation to solve the equations of momentum and mass transport; for very short wavelengths, however, convergence of the numerical scheme is slow and computation of dispersion coefficients has not been attempted.

The numerical results agree well with experimental data for dispersion in packed beds if an appropriate tube geometry is selected. This particular geometry has been determined by previous investigators interested in permeabilities of packed beds. For low Peclet numbers, the agreement between the model predictions and experimental data is especially good. These results indicate that two important transport properties of packed beds, permeability and dispersion, can be analyzed successfully with the same model pore structure. The present model has no mechanism for mass transport between adjacent flow channels and is therefore incapable of predicting radial dispersion.

BACKGROUND

Transport phenomena in model geometries have frequently been studied as a first step in understanding these phenomena in more complicated settings. Geometries used to describe transport in consolidated porous media often fall into one of two categories, the pore network theories (Saffman, 1960) and the constricted tube theories (Payatakes et al., 1973). More compex models of porous media have also been employed (Snyder and Stewart, 1966; Sorensen and Stewart, 1974; Zick and Homsy, 1982); the mathematical and numerical complexity increases accordingly. This paper focuses on time-dependent mass transport arising from flow in the constricted tube geometry. In particular, the problem of dispersion in a sinusoidal tube is studied using a rigorous approach based on asymptotic long-time solutions of the convective-diffusion equation. The analysis is an extension of the ideas proposed by Taylor (1953) and Aris (1956) in their examinations of dispersion in a straight cylindrical tube.

Fluid motion in sinusoidal tubes has been studied for both the creeping flow and low Reynolds number regimes (Chow and Soda, 1972; Fedkiw and Newman, 1977; Deiber and Schowalter, 1979; Neira and Payatakes, 1979). The hydrodynamic calculations have been used to predict permeabilities, steady-state mass transport (Fedkiw and Newman, 1977), and particle deposition (Payatakes et al., 1974) in porous media. The success of the calculations in predicting these properties has been fairly well established (Payatakes et al., 1973). Although more complicated models have been proposed, the sinusoidal tube geometry is the simplest geometry which incorporates the converging and diverging nature of actual porous media.

The earliest attempt to model the properties of porous media from a microscopic viewpoint was undertaken by Maxwell (1892). His study of the electrical conductivity of dilute suspensions of spheres is readily interpreted in terms of mass transport in the same setting. Unfortunately, his results are valid for porosities much higher than typically occur in consolidated porous media. Although these results can be extended to slightly lower porosities by sophisticated mathematical techniques (Jeffrey, 1973), a more general calculation of mass transport apparently must be done numerically. In any case, the analytical calculations are restricted to conditions for which the interstitial fluid is stagnant. Of more interest is the case where carrier fluid both transports and disperses solute. Only recently have attempts been made to use numerical methods on this more complicated problem. An analysis of dispersion during flow perpendicular to an array of cylinders was developed by Carbonell and Whitaker (1983), and Eidsath et al. (1983). Lee (1979) examined dispersion during flow through a regular array of spherical particles; his calculations failed, however, because of numerical difficulties. It was suggested by Lee that numerical calculations be applied first to simpler geometries than the one attempted—the sinusoidal tube appears to be a more tractable geometry.

METHOD OF MOMENTS ANALYSIS

A rigorous theory of the dispersion that results from convection and diffusion in spatially periodic porous media was recently developed by Brenner (1980). The theory follows the classical "method of moments" approach employed by Aris (1956) in describing dispersion in capillaries. Aris' analysis, however, is restricted to geometries for which flow is locally unidirectional; the extended method is applicable to a more general class of fluid motions occurring in media composed of periodic units. Of the problems falling into this category, perhaps the simplest arises from flow in a periodically constricted tube (PCT). A sinusoidal tube, Figure 1, is a specific PCT geometry generated by revolving the sine function about an axis of symmetry. The analysis presented below is a specific application of Brenner's general formalism to the sinusoidal geometry. A complete description of the method of moments analysis is lengthy, so only key points will be presented here. More detailed information can be found in the original article (Brenner, 1980).

Within each period of the sinusoidal tube, a system of local cylindrical coordinates is defined with variables r and z. An additional global variable, n, is used to identify a specific period, or unit cell, in the infinite tube. The values of n, r, and z uniquely define a spatial position in the domain of fluid motion. Using these coordinates, the convective-diffusive transport of a slug of tracer introduced at $n = 0$ and $z = 0$ can be described with the following equation:

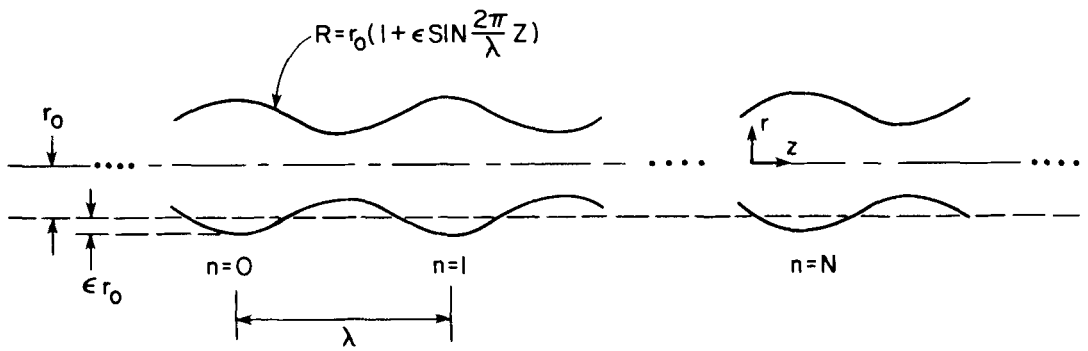

Figure 1. Sinusoidal tube model. A local coordinate system is defined within each unit cell. The global variable n extends to plus and minus infinity.

$$\frac{\partial P}{\partial t} + v_z \frac{\partial P}{\partial z} + v_r \frac{\partial P}{\partial r} = D \frac{\partial^2 P}{\partial z^2} + \frac{D}{r}\frac{\partial}{\partial r} r \frac{\partial P}{\partial r} + \frac{\delta(n)\delta(z)\delta(t)}{\pi r_o^2} \quad (1)$$

$$0 \leq z \leq \lambda$$
$$0 \leq r \leq R$$
$$-\infty \leq n \leq \infty$$

where

$$R = r_o \left[1 + \epsilon \sin\left(\frac{2\pi}{\lambda} z\right)\right] \quad (2)$$

P is the probability of finding a tracer particle in a volume element dV; D is the assumed isotropic diffusion coefficient; and λ, ϵ, and r_o define the wavelength, amplitude, and mean value, respectively, of the sine wave R which describes the wall. The radial and axial components of the fluid motion are given by v_r and v_z, and it is appropriate to represent the tracer pulse using the Dirac delta function, δ. As a consequence of the source term in Eq. 1, P satisfies the normalization condition,

$$1 = \sum_n \int_V P dV \quad (3)$$

where V is the volume of a single unit cell. Conditions associated with Eq. 1 are as follows:

1. Zero wall flux:

$$\boldsymbol{n} \cdot \nabla P = 0 \text{ on } R \quad (4)$$

where $\boldsymbol{n}$ is an outward normal vector on the tube wall.

2. Infinite axial boundaries:

$$P \to 0 \quad \text{as} \quad n \to \pm\infty. \quad (5)$$

3. Continuity of P across the boundary of cell n and cell $n+1$:

$$\left.\frac{\partial P_{n+1}}{\partial z}\right|_{z=0} = \left.\frac{\partial P_n}{\partial z}\right|_{z=\lambda} \quad (6)$$

where the subscripts are associated with an arbitrary unit cell and its neighbor.

Equations 4 and 5 are conventional boundary conditions for Eq. 1. The third condition replaces Eq. 5 when Eq. 1 is to be solved within a single unit cell using local coordinates alone. The interplay between local and global descriptions plays a crucial part in the analysis developed by Brenner.

The set of equations and boundary conditions listed above fully specify the transport of tracer in the tube; considerable simplification can be achieved by limiting attention to specific features of this problem. In many cases interest lies in the asymptotic long-time distribution of tracer. Within this regime it can be shown that Brownian motion has erased a tracer particle's "memory" of its initial local position. In other words, the initial values of r and z are no longer correlated with the present values of r and z. For the sinusoidal tube, the long-time assumption requires

$$t \gg \frac{r_o^2}{D} \quad (7)$$

and

$$t \gg \frac{\lambda^2}{D} \quad (8)$$

A further simplification arises when longitudinal transport is of primary interest; dispersion can be characterized by an axial distribution of locally-averaged concentrations. These concentrations, taken as a volume average over each unit cell, can be expressed as a function of n; the lower order moments of this function will provide detailed information concerning dispersion in the tube.

The simplifications described above are imposed through the application of "local" and "global" moment operators to the convective-diffusion equation and its boundary conditions. Local moments are defined,

$$\mu_m(z,r,t) = \sum_{n=-\infty}^{\infty} (\lambda n)^m P_n(z,r,t) \quad (9)$$

where m is an arbitrary integer greater than or equal to zero. Applying this operator to Eq. 1 yields a set of differential equations with m as a parameter,

$$\frac{\partial \mu_m}{\partial t} + v_z \frac{\partial \mu_m}{\partial z} + v_r \frac{\partial \mu_m}{\partial r} = D \frac{\partial^2 \mu_m}{\partial z^2} + \frac{D}{r}\frac{\partial}{\partial r} r \frac{\partial \mu_m}{\partial r} + \frac{\delta(m)\delta(z)\delta(t)}{\pi r_o^2} \quad (10)$$

It is important to note that each equation is written in purely local variables. The boundary conditions transform according to m; the lower order relationships are listed below:

$$[|\mu_0|] = 0 \quad (11)$$

$$[|\mu_1|] = -[|z\mu_0|] \quad (12)$$

$$[|\mu_2|] = \left[\left|\frac{\mu_1^2}{\mu_0}\right|\right] \quad (13)$$

$$\left[\left|\frac{\partial \mu_0}{\partial z}\right|\right] = 0 \quad (14)$$

$$\left[\left|\frac{\partial \mu_1}{\partial z}\right|\right] = -\left[\left|\frac{\partial (z\mu_0)}{\partial z}\right|\right] \quad (15)$$

$$\left[\left|\frac{\partial \mu_2}{\partial z}\right|\right] = \left[\left|\frac{\partial}{\partial z}\left(\frac{\mu_1^2}{\mu_0}\right)\right|\right] \quad (16)$$

where

$$[|f|] = f(\lambda,r) - f(0,r) \quad (17)$$

In the development here, only the three lowest order moments are necessary, $m = 0,1,2$.

It is helpful to define total moments with the following operator,

$$M_m(t) = \int_V \mu_m(z,r,t) dV \quad (18)$$

As before, V is the volume of a unit cell. The total moments, $M_m(t)$, are functions of time alone and can be found by solving fairly simple ordinary differential equations. Without going into details of their derivation, the following asymptotic long-time relationships involving the total moments can be obtained:

$$\frac{dM_1}{dt} = \overline{U} \quad (19)$$

$$\frac{dM_2}{dt} = 2\overline{U}^2 t + 2\overline{U}\,\overline{B} + \frac{2D}{V}\int_V \left[\left(\frac{\partial B}{\partial z}\right)^2 + \left(\frac{1}{r}\frac{\partial B}{\partial r}\right)^2\right] dV. \quad (20)$$

In these equations $\overline{U}$ is the average velocity in the tube, and $\overline{B}$ is the volume average of a function defined by,

$$\overline{U} + v_z \frac{\partial B}{\partial z} + v_r \frac{\partial B}{\partial r} = D \frac{\partial^2 B}{\partial z^2} + \frac{D}{r}\frac{\partial}{\partial r} r \frac{\partial B}{\partial r} \quad (21)$$

with

$$\boldsymbol{n} \cdot \nabla B = 0, \quad \text{on } R \quad (22)$$

$$[|B|] = -\lambda \quad (23)$$

$$\left[\left|\frac{\partial B}{\partial z}\right|\right] = 0 \quad (24)$$

Terms decreasing exponentially with time have been neglected in writing both Eqs. 19 and 20. Equation 19 confirms the intuitive notion that a neutrally buoyant point particle is transported through the tube with the average velocity of the fluid.

The dispersion coefficient for the sinusoidal tube is related to the axial moments of the tracer distribution. This relationship is given by Einstein's theory of Brownian motion,

$$2\zeta t = \overline{(n - \overline{n})^2} \quad (25)$$

$$= M_2 - M_1^2 \quad (26)$$

where ζ is the axial dispersion coefficient, and overbars indicate

a mean value. Combining Eqs. 19, 20, and 26, the dispersion coefficient can be written,

$$\zeta = \frac{D}{V}\int_V \left[\left(\frac{\partial B}{\partial z}\right)^2 + \left(\frac{1}{r}\frac{\partial B}{\partial r}\right)^2\right] dV \tag{27}$$

The calculation of the dispersion coefficient has thus been reduced to the solution of Eqs. 21–24 and subsequent evaluation of Eq. 27. The major result of the entire analysis is reduction of a partial differential equation in three variables in an infinite domain (Eq. 1) to an equation in two local variables in a finite domain (Eq. 21).

DISPERSION IN TUBES WITH LONG WAVELENGTHS

The preceding analysis provides a more tractable description of mass transport in a sinusoidal tube than the complete convective-diffusion equation. The dispersion problem has been reduced to three distinct calculations: determination of the velocity profile, computation of B, and evaluation of the integral in Eq. 27. The resulting dispersion coefficient, made dimensionless with the diffusion coefficient, will be a function of the dimensionless amplitude, the dimensionless wavelength, and the Peclet number: ϵ, $\lambda^* = \lambda/r_o$, and $Pe = \overline{U}\lambda/D$, respectively. For arbitrary values of these parameters, all three calculations must be done numerically. For the asymptotic case of large λ^*, however, analytical expressions for the dispersion coefficient have been found. These solutions are described below.

At low Reynolds numbers the fluid motion in the tube is governed by the equation,

$$E^4\psi = 0 \tag{28}$$

where

$$E^2 = \frac{\partial^2}{\partial r^2} - \frac{1}{r}\frac{\partial}{\partial r} + \frac{\partial^2}{\partial z^2} \tag{29}$$

The stream function ψ is related to the axial and radial components of fluid motion in cylindrical coordinates:

$$v_z = -\frac{1}{r}\frac{\partial \psi}{\partial r} \tag{30}$$

$$v_r = \frac{1}{r}\frac{\partial \psi}{\partial z} \tag{31}$$

When applying Eq. 28 to a single unit cell within the tube, the following boundary conditions are considered:

1. No slip at the wall:

$$\frac{\partial \psi}{\partial r} = \frac{\partial \psi}{\partial z} = 0, \qquad \text{at } r = R \tag{32}$$

2. Finite velocities at the tube centerline:

$$\frac{\partial \psi}{\partial r} = \frac{\partial \psi}{\partial z} = 0, \qquad \text{at } r = 0 \tag{33}$$

3. Periodic motion:

$$\frac{\partial^n \psi(r,0)}{\partial z^n} = \frac{\partial^n \psi(r,\lambda)}{\partial z^n} \tag{34}$$

In addition, ψ is arbitrarily set to 0 along the centerline. Since the axial flux is constant, the value of ψ at the wall is fixed.

$$\psi = -\frac{r_o^2}{2}\overline{V}_z, \qquad \text{at } r = R \tag{35}$$

Here $\overline{V}_z$ is the mean velocity in the tube at $z = 0$. This value is not the same as the mean velocity in the tube, $\overline{U}$. The two quantities are related by the equation,

$$\overline{U} = \frac{\overline{V}_z}{(1 + \epsilon^2/2)} \tag{36}$$

For large values of λ^*, the solution to Eq. 28 can be written as a perturbation expansion (Chow and Soda, 1972),

$$\psi = \sum_{j=0}^{N}\left(\frac{1}{\lambda^*}\right)^j \psi_j \tag{37}$$

Solving for the first two terms in the expansion using regular perturbation theory, ψ can be approximated to order λ^{*-2},

$$\psi = \frac{1}{2}\left[\left(\frac{r}{R}\right)^4 - 2\left(\frac{r}{R}\right)^2\right] \tag{38}$$

From Eq. 37, v_r and v_z are easily obtained,

$$v_r = 0 + 0(\lambda^{*-1}) \tag{39}$$

$$v_z = 2\overline{V}_z\left(\frac{r_o}{R}\right)^2\left[1 - \left(\frac{r}{R}\right)^2\right] + 0(\lambda^{*-2}) \tag{40}$$

For large values of λ^* the flow in the tube is essentially unidirectional. For this reason, the zero order approximation could have been obtained in an alternative fashion using "lubrication" theory.

Approximating the convective terms with the velocity profiles presented in Eqs. 39 and 40, the differential equation for B can be written,

$$\overline{U} + 2\overline{V}_z\left(\frac{r_o}{R}\right)^2\left[1 - \left(\frac{r}{R}\right)^2\right]\frac{\partial B}{\partial z} = D\frac{\partial^2 B}{\partial z^2} + \frac{D}{r}\frac{\partial}{\partial r}r\frac{\partial B}{\partial r} \tag{41}$$

For large values of λ^*, the boundary conditions are,

$$\frac{\partial B}{\partial r} = 0, \qquad \text{at } r = R \tag{42}$$

$$B(\lambda,r) - B(0,r) = -\lambda \tag{43}$$

$$\frac{\partial B(\lambda,r)}{\partial z} = \frac{\partial B(0,r)}{\partial z} \tag{44}$$

The general solution to Eqs. 41–44 is still quite difficult; it is convenient to use the solution for a straight cylindrical tube as a base case (Brenner, 1980).

$$B = \frac{\overline{U}r_o^2}{8D}\left[\left(\frac{r}{r_o}\right)^4 - 2\left(\frac{r}{r_o}\right)^2\right] - z. \tag{45}$$

In the spirit of lubrication theory, the base case is used to generate a trial solution of the form:

$$B = \frac{\overline{U}R^2}{8D}\left[\left(\frac{r}{R}\right)^4 - 2\left(\frac{r}{R}\right)^2\right] - f(z) \tag{46}$$

Substitution of this function into Eq. 41 yields a solution consistent with the previous approximations if $f(z)$ is chosen of the form

$$f(z) = z - \left[\frac{1}{1 + \epsilon^2/2}\right]\left[\frac{\epsilon\lambda}{\pi}\cos\left(\frac{2\pi}{\lambda}z\right) + \frac{\epsilon^2\lambda}{8\pi}\sin\left(\frac{4\pi}{\lambda}z\right)\right] \tag{47}$$

Omitted terms have the order Pe/λ^{*2} and Pe^{-1}. Evaluation of Eq. 27 using Eqs. 46 and 47 yields the dimensionless dispersion coefficient,

$$\frac{\zeta}{D} = \frac{1}{(1 + \epsilon^2/2)^3}\left[1 + \frac{15}{2}\epsilon + \frac{45}{8}\epsilon^4 + \frac{5}{16}\epsilon^6\right] + \left[\frac{\overline{U}r_o}{D}\right]^2\left[\frac{1}{48(1 + \epsilon^2/2)}\right]\left[1 + 3\epsilon^2 + \frac{3}{8}\epsilon^4\right] \tag{48}$$

Since Eq. 48 describes dispersion under conditions for which the flow is essentially unidirectional, the dispersion coefficient could have been obtained by modification of the Taylor-Aris theory. The alternate derivation is briefly outlined here: A cylindrical tube dispersion coefficient is written in terms of the local sinusoidal radius. This dispersion coefficient is then transformed into an axially dependent variance of residence time. Recognizing that residence times along the tube are additive, the local variance function can be integrated to obtain an overall time variance for an entire unit cell. When this time variance is rewritten as a dispersion coefficient, the result is Eq. 48. This nonrigorous approach cannot be extended to more general sinusoidal tube geometries for which flow is not unidirectional.

A long-wavelength solution can also be found when Pe is small. Under these conditions Eq. 41 and its boundary conditions reduce to the simple form:

$$\frac{\partial^2 B}{\partial z^2} + \frac{1}{r}\frac{\partial}{\partial r} r \frac{\partial B}{\partial r} = 0 \tag{49}$$

$$B(\lambda,r) - B(0,r) = -\lambda \tag{50}$$

$$\frac{\partial B}{\partial z}(\lambda,r) = \frac{\partial B}{\partial z}(0,r) \tag{51}$$

$$\boldsymbol{n} \cdot \nabla \mathrm{B} = 0, \qquad \text{on } r = R \tag{52}$$

The solution to this problem is easily found by perturbation methods.

$$B = -\int_0^z \frac{(1-\epsilon)^{3/2}}{(1+\epsilon \sin(2\pi/\lambda)z)^2} dz + \lambda \cdot 0\left(\frac{r_o}{\lambda}\right) \tag{53}$$

This equation in turn yields the low Peclet dispersion coefficient,

$$\frac{\zeta}{D} = \frac{(1-\epsilon^2)^{3/2}}{(1+\epsilon^2/2)} + 0(\lambda^{*-1}) \tag{54}$$

This expression is equivalent to Eq. 6.2-12 in Giddings (1965).

In summary, dispersion coefficients in sinusoidal tubes with long wavelengths can be calculated at low and high *Pe* using Eqs. 48 and 54. Although the equations are applicable only in rather limited regimes, these conditions are not experimentally unattainable. The most important use of these calculations will be as a check of the numerical scheme described in the next section. It should be noted that Eqs. 48 and 54 properly reduce to the dispersion coefficient calculated by Aris (1956) for a straight tube with $\epsilon = 0$.

NUMERICAL SOLUTION OF METHOD OF MOMENTS PROBLEM

With numerical methods it is possible to compute dispersion coefficents over a range of Peclet numbers and tube geometries for which Eqs. 48 and 54 are inapplicable. The first step in the numerical procedure is calculation of the velocity profile. As mentioned before, several authors have analyzed low Reynolds number flow in sinusoidal tubes; the approach outlined here is nearly identical to the one described by Neira and Payatakes (1979). The equation for the stream function is first transformed to a rectangular coordinate system defined by:

$$\chi = \frac{r}{R} \tag{55}$$

and

$$\eta = \frac{z}{\lambda} \tag{56}$$

The proposed trial function expansion for ψ can then be expressed in terms of transformed variables,

$$\psi = \frac{1}{2}(\chi^4 - 2\chi^2) + \sum_{j=1}^{N_z}\sum_{i=1}^{N_R} C_{ij}\chi^2(1-\chi)^{i+1} \times \cos[2\pi(j-1)(\eta - 1/4)] \tag{57}$$

where the coefficients C_{ij} are to be determined by collocation. This expansion satisfies all boundary conditions for ψ exactly. The first term is equivalent to the lubrication approximation for flow described in the previous section. Substitution of the expansion for ψ into the transformed form of Eq. 28 yields a set of $N_z \times N_R$ equations containing $N_z \times N_r$ unknown coefficients. These coefficients are determined by setting the residuals to zero on a grid of collocation points defined by

$$\chi_i = \text{roots of } P_{N_R}^{0,0}(\chi), \qquad 0 < \chi < 1 \tag{58}$$

and

$$\eta_j = \frac{(j-1/4)}{2N_z} + \frac{1}{4}, \qquad \text{for } j = 1,2,\ldots,N_z \tag{59}$$

In Eq. 58, $P_{N_R}^{0,0}$ is the Jacobi polynomial of degree N_R with $\alpha = 0$ and $\beta = 0$. Once the coefficients have been calculated, the velocity profile is easily determined as a function of C_{ij} by differentiation of the expansion for χ. The coefficients C_{ij}, and therefore the velocity profile, will be different for each different tube geometry. Since flow in sinusoidal tubes has been described by a number of authors, a discussion of the solution will not be presented here. Using an 8×8 collocation grid, the results of the present study are in excellent agreement with those of Fedkiw and Newman (1977).

The numerical solution of the equation for B is obtained by a series of calculations similar to those used in obtaining the velocity field. Equations 21-24 are first transformed to the χ and η coordinate system. Using the equation for B in a straight cylindrical tube as a base case, the following trial function expansion is proposed:

$$B = \frac{PeR^2}{8\lambda^2}[\chi^4 - 2\chi^2] - \eta + \sum_{\substack{i,j \\ \text{not both zero}}}^{N_z}\sum_{i=0}^{N_R} R(\chi,i)A(\eta,i,j) + C_{00}\eta(1-2\eta)(1-\eta) \tag{60}$$

where

$$R(\chi,i) = \chi^2(1-\chi)^{i-1} \tag{61}$$

and

$$A(\eta,i,j) = C_{ij}\sin 2\pi jn + D_{ij}\cos 2\pi jn. \tag{62}$$

In Eq. 62, C_{ij} and D_{ij} are the unknown coefficients to be determined by collocation.

The form of the expansion for B follows from the nature of Eq. 21, which defines this quantity. Both sine and cosine terms are included in the expansion since the equation has a "direction" associated with its convective terms. This contrasts with the expansion for ψ which has symmetry about the plane $\eta = 1/4$. In addition to its asymmetry, Eq. 21 defines B only to within an arbitrary constant. This forces the summation in Eq. 60 to exclude the $i,j = 0$ term. In order to include the correct number of constants, a function of η is placed outside the summation. This function, which satisfies the appropriate boundary conditions, is linearly independent of the set of terms in the summation. Its coefficient, C_{00}, can therefore be determined in the same manner as the other unknown coefficients.

Collocation points are chosen by:

$$\eta_j = \frac{j+1}{2(N_z+1)}, \qquad j = 0,1,\ldots,2N_z \tag{63}$$

and

$$\chi_i = \text{roots of } P_{N_R}^{0,0},\chi \qquad 0 < \chi < 1 \tag{64}$$

The points on the boundary are necessary since the expansion for B does not satisfy the wall boundary condition exactly. The expansion generates $(2N_z+1) \times (N_R+1)$ unknowns which can be evaluated using the $(2N_z+1) \times (N_R+1)$ collocation points. (Note: the coefficients C_{i0} are identically zero for all values of i greater than 0.) These unknown coefficients are calculated by substituting the expansion for B into Eq. 21, or into Eq. 22 for boundary points, and setting the residual equal to zero. The function B is now determined as a function of position, and the evaluation of the integral which relates B to the dispersion coefficient is the only calculation remaining. This integral is evaluated using 24-point Gauss-Legendre quadrature in the χ and η coordinate system.

DISCUSSION OF NUMERICAL SOLUTION

As mentioned previously, the dimensionless dispersion coefficient in a sinusoidal tube will be a function of λ^*, ϵ, and *Pe*. Figure 2 shows the dependence of the dispersion coefficient on λ^* for fixed ϵ and *Pe*. The parameters have been selected so that when wavelengths are large, the conditions for Eq. 48 are satisfied and overlap of the numerical and analytical solutions is observed. For smaller

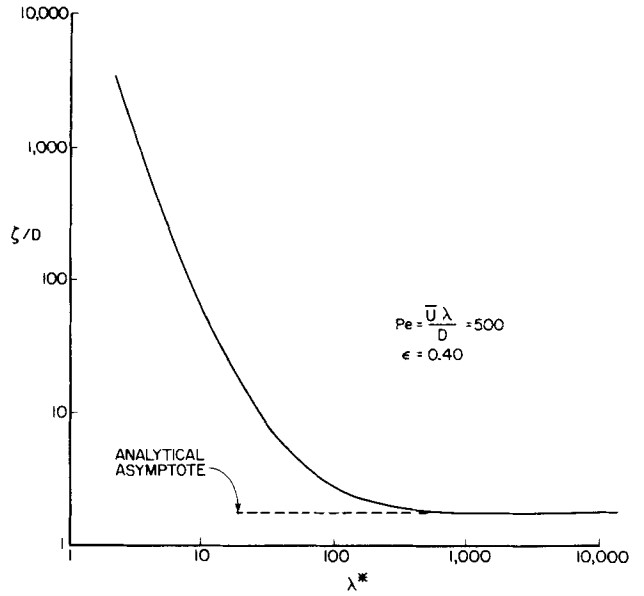

Figure 2. Dimensionless dispersion coefficient as a function of dimensionless wavelength. The value of the long wavelength asymptote is given by Eq. 48.

wavelengths, radial flow becomes important and the dispersion coefficient increases. Under conditions for which the asymptotic behavior of Eq. 53 is valid, small Pe and large λ^*, similar agreement of analytical and numerical solutions is observed.

Figure 3 presents the dependence of ζ on Pe when ϵ and λ^* are chosen as 0.40 and 3.33, respectively, values which successfully correlate permeability data for a packed bed of spheres using the sinusoidal tube model (Payatakes et al., 1973; Fedkiw and Newman, 1977). For small Pe the dimensionless dispersion coefficient is governed by diffusion and can be correlation by geometrical parameters alone. This behavior is observed in Figure 3; the limiting dispersion coefficient is $0.647D$. As Pe is increased, a transition to convective mass transport is reflected in an increase in ζ. For very large Pe the dispersion coefficient satisfies the relationship,

$$\frac{\zeta}{D} = 0.0104 Pe^{1.88} \tag{65}$$

extremely well.

If one models a packed bed of spheres as an array of parallel sinusoidal tubes, the dispersion coefficient in the bed is the same as in each tube individually. The average tube velocity, $\overline{U}$, is related to the superficial bed velocity, V_s, by

$$\overline{U} = \frac{V_s}{\phi}, \tag{66}$$

where ϕ is the porosity of the bed. Dispersion coefficients in packed beds are commonly correlated using a Peclet number defined with the mean interstitial velocity, now identified as $\overline{U}$, and the mean particle diameter. This diameter is closely related to the sinusoidal wavelength and, to first approximation, will have the same value. These arguments lead to the conclusion that the sinusoidal tube Peclet number, Pe, is equivalent to the particle Peclet number for the packed bed. Therefore, experimental data for dispersion in these beds can be directly compared to Figure 3. When making this comparison it should again be emphasized that the sinusoidal tube model does not incorporate all of the phenomena that affect dispersion in packed beds. It is expected that imperfect packing and transport between adjacent flow channels may have a significant influence on dispersion. Figure 3 displays the correspondence of the current model to an empirical correlation prepared by Hiby (1962). The agreement is surprisingly good for Pe less than 100. Particularly encouraging is the agreement in low Pe number asymptotes for the dispersion coefficient; Hiby's result, $0.67D$, is nearly the result of the current model. Hiby's data seem the most carefully prepared of the data sets encountered. Most dispersion data (Bear, 1972; Wen and Fan, 1975) will not correlate with the present analysis as well. The low Pe result, however, is the same throughout the works surveyed.

The sensitivity of the numerically computed dispersion coefficient to tube geometry is displayed in Figures 4, 5, 6, and 7. Examination of Figure 4 reveals that at low Pe the dispersion coefficient is relatively independent of wavelength, but this is certainly not the behavior observed in the high Pe regime. As expected, at low Pe the effect of shorter wavelengths is a decrease in dispersion coefficient, and at high Pe, an increase. In Figure 5 one observes that the strongest influence of wall amplitude occurs in the diffusion-dominated regime at low Pe. Figures 6 and 7 display the dependence of ζ/D on both λ^* and ϵ in a different fashion than Figures 4 and 5. Figure 6 shows that as the wall amplitude is decreased, the dispersion coefficient tends toward the Taylor result for straight tubes; as the wall amplitude is increased toward 1.0, the value at which the tube is "pinched off", the value of ζ/D grows to a value approximately an order of magnitude larger (for the chosen value of λ^*). Figure 7 shows a similar plot of the dependence of the dispersion coefficient on λ^*. For values of λ^* less than 5, the dispersion coefficient is a strong function of wavelength. At very small wavelengths recirculation occurs and dispersion in-

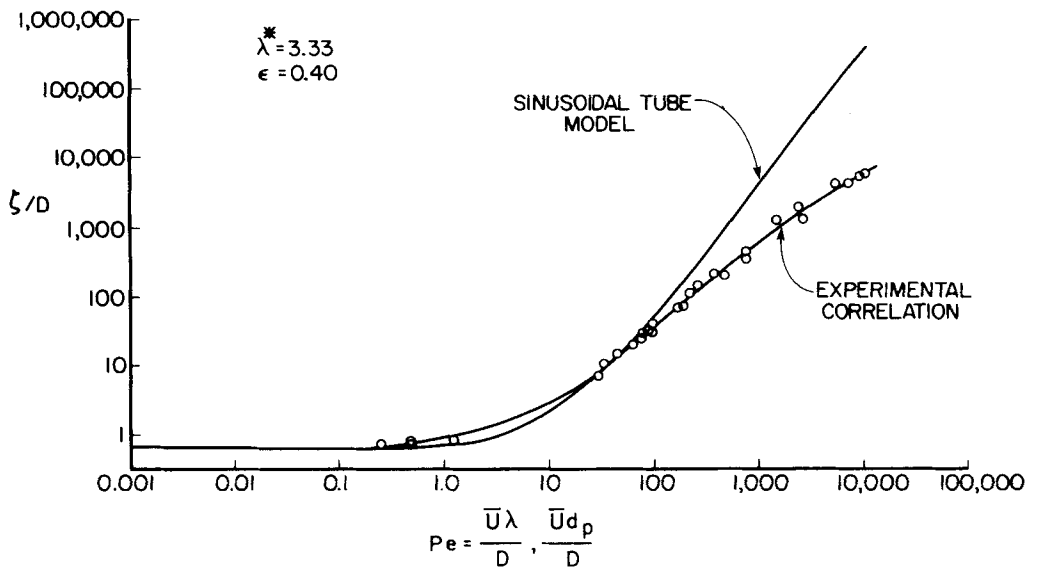

Figure 3. Dimensionless dispersion coefficient as a function of Peclet number; comparison of sinusoidal tube model to experimental data. The data and correlation are from Hiby (1972). Hiby's correlation is expressed in terms of a Peclet number defined with the mean particle diameter.

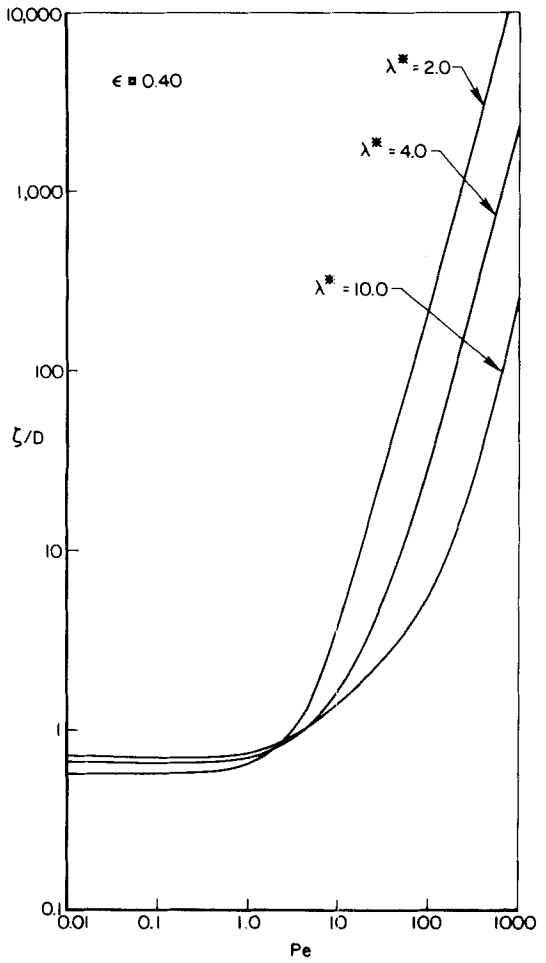

Figure 4. Dimensionless dispersion coefficient as a function of Peclet number. The various curves correspond to different values of the dimensionless wavelength $\lambda^*(=\lambda/r_D)$. In the low *Pe* regime ζ/D is insensitive to λ^*, but this is not true in the convectively dominated regime where $Pe \gg 1$.

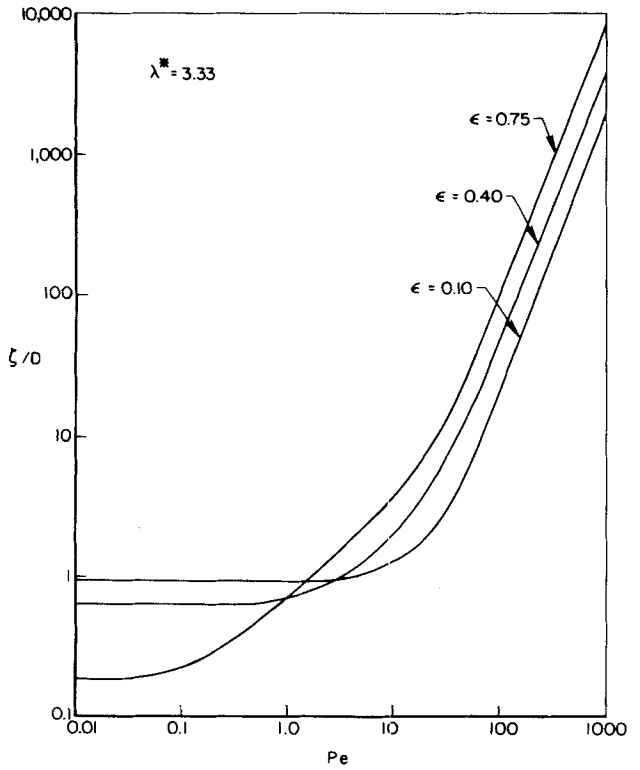

Figure 5. Dimensionless dispersion coefficient as a function of *Pe* with wall amplitude ϵ as a parameter. This figure is similar to Figure 4 except that the value of ζ/D is very sensitive to ϵ at low *Pe*.

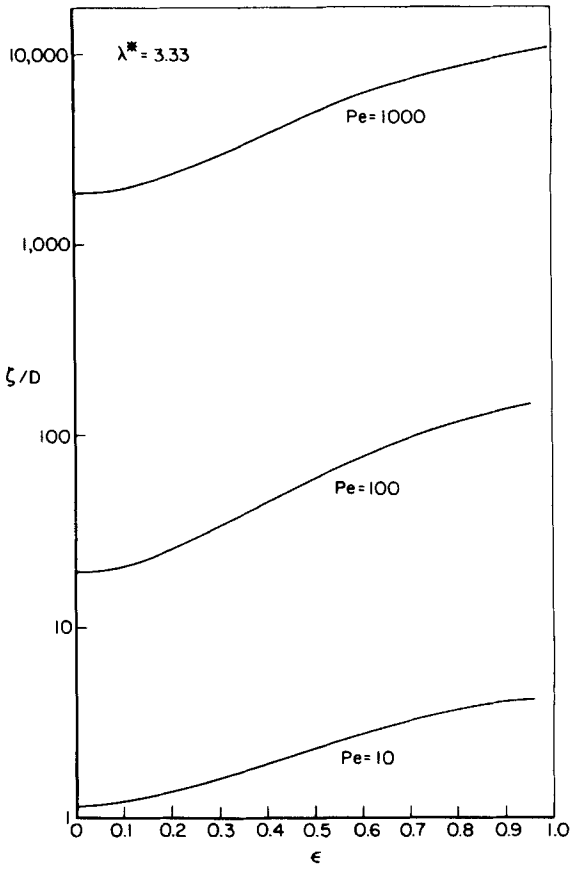

Figure 6. Dispersion coefficient as a function of wall amplitude ϵ. The intercept at $\epsilon = 0$ agrees with the Taylor result for straight tubes. At $\epsilon = 1.0$ the tube is completely constricted by the converging walls.

creases dramatically. It should be noted that the numerical scheme is successful in flows with recirculation and regions of closed streamlines. A comparison of the numerical results to the data presented in Figure 3 confirms the notion that the parameters fit by permeability data also give a good correlation to dispersion data.

A major objection to the sinusoidal tube model for dispersion is the absence of transverse mass and momentum transport. Without considering a more complicated model, it would be difficult to incorporate such effects. Higher order models of dispersion in packed beds will probably begin with actual bed structure and incorporate complete solutions of the equations of motion. These calculations will be considerably more difficult than those described in the present work. (Results of this type have recently been obtained by Eidsath et al., 1983). The difficulty is illustrated by the failure of the computations by Lee (1979). Velocity profiles in complicated bed structures are available (Snyder and Stewart, 1966; Sorensen and Stewart, 1974), however, and it is expected that these profiles will eventually be used successfully in analyses similar to the present one. The most important arguments in favor of the sinusoidal tube model for porous media are its simplicity and its relatively good agreement with experimental data.

ACKNOWLEDGMENTS

Funding for this work has been provided by the National Science Foundation (CPE80-03320) and the Dow Chemical Company. Special thanks are in order to Professor S. Sundaresan for his invaluable assistance on numerical techniques.

NOTATION

$B,\overline{B}$ = function defined by Eqs. 21-24, and its volume average, respectively

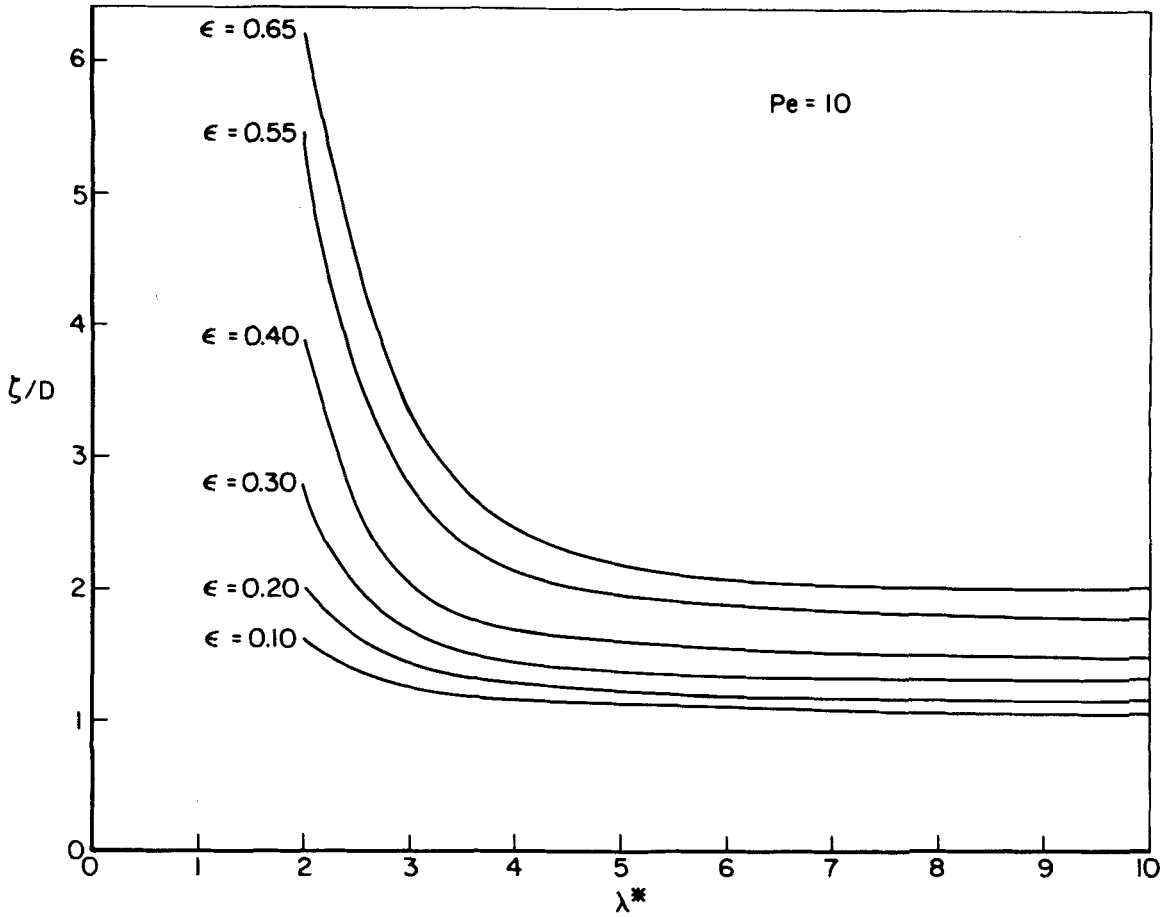

Figure 7. Dispersion coefficient as a function of wavelength of wall. Recirculating flows were observed under some of the conditions examined in the figure. As λ* is decreased below 2.0 the numerical scheme converges slowly and further computation was not attempted.

d_p = mean particle diameter in a packed bed
D = solute diffusion coefficient
C_{ij}, D_{ij} = collocation expansion coefficients
m = arbitrary integer
M_m = the mth total moment defined by Eq. 18
$n, \bar{n}$ = global coordinate (Figure 1) and its mean value as weighted by the solute distribution
n = outward normal of the tube wall
N_R, N_z = number of radial and axial terms in the collocation expansion
P, P_n = probability of finding a solute particle in a volume element dV, and this value in cell n, respectively
$P_{N_R}^{0,0}$ = Jacobi polynomial of degree N_R with parameters $\alpha = 0$ and $\beta = 0$
Pe = Peclet number = $\overline{U}\lambda/D$
r = local radial coordinate
r_o = mean wall radius (Figure 1)
R = $r_o(1 + \epsilon \sin(2\pi/\lambda)z)$
t = time span after solute introduced into tube
$\overline{U}$ = mean volume-averaged axial velocity
v_r, v_z = radial and axial velocity components
V = volume of a unit cell
V_s = superficial bed velocity
$\overline{V}_z$ = mean axial velocity at plane $z = 0$
z = local axial coordinate

Greek Letters

δ = Dirac delta function
ϵ = dimensionless sine function amplitude (Figure 1)
η = dimensionless axial coordinate = z/λ
λ = wavelength of sine function (Figure 1)
λ^* = dimensionless wavelength of sine function = λ/r_o
μ_m = mth local moment defined by Eq. 9
ζ = dispersion coefficient
ϕ = porosity of porous medium
χ = dimensionless radial coordinate = r/R
ψ, ψ_j = stream function, and the jth term in the expansion for the stream function (Eq. 37), respectively

LITERATURE CITED

Aris, R., "On the Dispersion of a Solute in a Fluid Flowing Through a Tube," *Proc. Roy. Soc.*, **A235**, 67, London (1956).

Bear, J., *Dynamics of Fluids in Porous Media*, American Elsevier, New York (1972).

Brenner, H., "Dispersion Resulting from Flow Through Spatially Periodic Porous Media," *Phil., Trans. Roy. Soc.*, **297**, 81, London (1980).

Carbonell, R. G., and S. Whitaker, "Dispersion in Pulsed Systems. II: Theoretical Developments For Passive Dispersion in Porous Media," *Chem. Eng. Sci.* **38**, 1795 (1983).

Chow, J. C. F., and K. Soda, "Laminar Flow in Tubes with Constriction," *Phys. Fluids*, **15**, 700 (1972).

Deiber, J. A., and W. R. Schowalter, "Flow Through Tubes with Sinusoidal Axial Variations in Diameter," *AIChE J.*, **25**, 638 (1979).

Eidsath, A., et al., "Dispersion in Pulsed Systems. III: Comparison between Theory and Experiments for Packed Beds," *Chem. Eng. Sci.*, **38**, 1803 (1983).

Fedkiw, P., and J. Newman, "Mass Transfer at High Peclet Numbers for Creeping Flow in a Packed-Bed Reactor," *AIChE J.*, **23**, 255 (1977).

Giddings, J. C. *Dynamics of Chromatography. Part 1. Principles and Theory*, Marcel Dekker, Inc., New York (1965).

Hiby, J. W., "Longitudinal and Transverse Mixing During Single-Phase Flow Through Granular Beds," Symp. Interactions Between Fluids and Particles, *Inst. Chem. Eng.*, 312, London (1962).

Jeffrey, D. J., "Conduction Through a Random Suspension of Spheres," *Proc. Roy. Soc.* **A335**, 355, London (1973).

Lee, H., "Analysis of Pseudo-Continuum Mass Transfer in Media with Spatially Periodic Boundaries," *Chem. Eng. Sci.*, **34**, 503 (1979).

Maxwell, J. C., *A Treatise on Electricity and Magnetism*, V. I, 3rd Ed., Clarendon Press, Oxford (1892).
Neira, M. A., and A. C. Payatakes, "Collocation Solution of Creeping Newtonian Flow Through Sinusoidal Tubes," *AIChE J.*, **25**, 725 (1979).
Payatakes, A. C., Chi Tien, and M. R. Turian, "A New Model for Granular Porous Media. 1: Model Formulation," *AIChE J.*, **19**, 58 (1973).
——, "Trajectory Calculation of Particle Deposition in Deep Bed Filtration. 1: Model Formulation," *AIChE J.*, **20**, 889 (1974).
Saffman, P. G., "Dispersion Due to Molecular Diffusion and Macroscopic Mixing in Flow Through a Network of Capillaries," *J. Fluid Mech.*, **7**, 194 (1960).
Snyder, L. J., and W. E. Stewart, "Velocity and Pressure Profiles for Newtonian Creeping Flow in Regular Packed Beds of Spheres," *AIChE J.*, **12**, 167 (1966).
Sorensen, J. P., and W. E. Stewart, "Computation of Forced Convection in Slow Flow through Ducts and Packed Beds. II: Velocity Profile in a Simple Cubic Array of Spheres," *Chem. Eng. Sci.*, **29**, 819 (1974).
Taylor, G. I., "The Dispersion of Soluble Matter in Solvent Flowing Slowly Through a Tube," *Proc. Roy. Soc.*, **219**, 186, London (1953).
Wen, C. Y., and L. T. Fan, *Models for Flow Systems and Chemical Reactors*, Marcel Dekker, Inc., New York (1975).
Zick, A. A., and G. M. Homsy, "Stokes Flow through Periodic Arrays of Spheres," *J. Fluid Mech.*, **115**, 13 (1982).

Manuscript received January 26, 1983; revision received December 6, 1983, and accepted December 8.

A Heat Transfer Model for Tubes Immersed in Gas Fluidized Beds

A model for local heat transfer between a gas-fluidized bed and a submerged tube is proposed based on combined dense-phase and lean-phase transport. The heat transfer process during dense-phase contact at the tube surface is modeled by packet renewal mechanism and the transfer process during lean-phase contact by fluid convection mechanism. The model predictions show good agreement with experimental local and average heat transfer coefficient data for horizontal tubes.

R. CHANDRAN
Department of Mechanical Engineering
Ohio University
Athens, OH 45701
and
J. C. CHEN
Department of Chemical Engineering
Lehigh University
Bethlehem, PA 18015

SCOPE

Many applications of fluidized beds involve heat transfer to or from immersed tubes and tube bundles. The rate of heat transfer between a fluidized bed and a submerged tube depends upon a number of factors, including the properties of the bed material and the contact fluid, bed and tube geometries, and the fluidization state. Measurements of heat transfer between fluidized beds and immersed tubes have been carried out by many investigators and both experimental data and correlations are reported in the literature. Reviews of the work are given by Gelperin and Einstein (1971), Gutfinger and Abuaf (1974), Zabrodsky et al. (1976), and Saxena et al. (1978). Comparisons of design correlations for bed-to-tube heat transfer coefficient are presented in Ainshtein and Gelperin (1966), Chen (1976), Grewal and Saxena (1980, 1981), and Botterill et al. (1981). However, from an application standpoint, there still is a need for improved phenomenological understanding of the mechanisms and appropriate modeling of the transport processes.

The foregoing remarks are especially true for tubes placed horizontally in fluidized beds. Since the fluid flow is in a direction normal to the tube axis for horizontal tubes, it is incorrect to assume axial symmetry. Local heat transfer coefficients could, and indeed do, vary with circumferential position on the tube surface. A few studies (Gelperin et al., 1966; Berg and Baskakov, 1974; Chandran et al., 1980) have reported local measurements around horizontal tubes. However, correlations for local heat transfer coefficient do not seem to have been published to date.

The objective of this study was to develop a mechanistic model for the prediction of local heat transfer coefficients, using information on bed-surface contact dynamics from fluid mechanics investigations (Chandran and Chen, 1982).

CONCLUSIONS AND SIGNIFICANCE

The local heat transfer coefficient at the tube surface was expressed as a weighted average of the dense-phase and the lean-phase transfer coefficients. For the case of negligible radiant contribution, heat transfer during dense-phase contact was attributed to the surface renewal mechanism and was modeled as a transient conduction process. Heat transfer during lean-phase contact was postulated to occur by the fluid convection mechanism with attendant enhancement due to the presence of particles in the medium.

With input data on local fluidization parameters, the model was able to successfully predict both local and average heat transfer coefficients for a wide range of test conditions.

Correspondence concerning this paper should be addressed to R. Chandran.